The Journal of Immunology

Proinflammatory S100 Proteins Regulate the Accumulation of Myeloid-Derived Suppressor Cells

Pratima Sinha, Chinonyerem Okoro, Dirk Foell, Hudson H. Freeze, Suzanne Ostrand-Rosenberg and Geetha Srikrishna

J Immunol 2008; 181:4666-4675; ;
doi: 10.4049/jimmunol.181.7.4666
http://www.jimmunol.org/content/181/7/4666

The Journal of Immunology is published twice each month by
The American Association of Immunologists, Inc.,
1451 Rockville Pike, Suite 650, Rockville, MD 20852

Print ISSN: 0022-1767 Online ISSN: 1550-6606.

Proinflammatory S100 Proteins Regulate the Accumulation of Myeloid-Derived Suppressor Cells[1]

Pratima Sinha,* Chinonyerem Okoro,* Dirk Foell,† Hudson H. Freeze,‡ Suzanne Ostrand-Rosenberg,[2]* and Geetha Srikrishna‡

Chronic inflammation is a complex process that promotes carcinogenesis and tumor progression; however, the mechanisms by which specific inflammatory mediators contribute to tumor growth remain unclear. We and others recently demonstrated that the inflammatory mediators IL-1β, IL-6, and PGE_2 induce accumulation of myeloid-derived suppressor cells (MDSC) in tumor-bearing individuals. MDSC impair tumor immunity and thereby facilitate carcinogenesis and tumor progression by inhibiting T and NK cell activation, and by polarizing immunity toward a tumor-promoting type 2 phenotype. We now show that this population of immature myeloid cells induced by a given tumor share a common phenotype regardless of their in vivo location (bone marrow, spleen, blood, or tumor site), and that $Gr1^{high}CD11b^{high}F4/80^{-}CD80^{+}IL4R\alpha^{+/-}Arginase^{+}$ MDSC are induced by the proinflammatory proteins S100A8/A9. S100A8/A9 proteins bind to carboxylated N-glycans expressed on the receptor for advanced glycation end-products and other cell surface glycoprotein receptors on MDSC, signal through the NF-κB pathway, and promote MDSC migration. MDSC also synthesize and secrete S100A8/A9 proteins that accumulate in the serum of tumor-bearing mice, and in vivo blocking of S100A8/A9 binding to MDSC using an anti-carboxylated glycan Ab reduces MDSC levels in blood and secondary lymphoid organs in mice with metastatic disease. Therefore, the S100 family of inflammatory mediators serves as an autocrine feedback loop that sustains accumulation of MDSC. Since S100A8/A9 activation of MDSC is through the NF-κB signaling pathway, drugs that target this pathway may reduce MDSC levels and be useful therapeutic agents in conjunction with active immunotherapy in cancer patients. *The Journal of Immunology,* **2008, 181: 4666–4675.**

Chronic inflammation increases the risk for the development of transformed cells and aggravates the development of established malignancies (1, 2). Some of the properties of inflammation that contribute to these processes are understood, such as the promotion of angiogenesis (3), the induction of tumor-promoting cytokines (4), the up-regulation of anti-apoptotic genes (5), and uncontrolled feed-forward signaling in tumor cells through cell surface receptors such as the receptor for advanced glycation end-products (RAGE)[3] (6). Many of these mechanisms are due to perturbations in the tumor microenvironment that co-opt innate immunity to favor tumor initiation and progression (7). We (8–10), and others (11, 12), recently reported that inflammation also promotes tumor progression by blocking adaptive immunity through the induction of myeloid-derived suppressor cells (MDSC), which prevent the activation of $CD4^+$ and $CD8^+$ T cells. The inflammatory stimuli in these studies were either the proinflammatory cytokines IL-1β and IL-6, or PGE_2. In these studies, mice with heightened levels of IL-1β or IL-6 in the tumor microenvironment accumulated MDSC with enhanced suppressive activity (8, 9, 11), and bone marrow stem cells cultured with PGE_2 or other E-prostanoid receptor agonists differentiated into MDSC (10). However, MDSC also accumulated in the absence of overtly elevated levels of IL-1β, IL-6, or PGE_2, suggesting that there may be additional inflammatory mediators that induce the accumulation and retention of MDSC.

Three members of the S100 family of calcium binding proteins, S100A12, S100A8, and S100A9, are inflammatory mediators released by cells of myeloid origin. These intracellular molecules are released to extracellular compartments in response to cell damage, infection, or inflammation, and function as proinflammatory danger signals (13–15). Elevated serum levels of S100A8 and S100A9 proteins are hallmarks of inflammatory disorders and recurrent infections (16), and increased S100A8 and S100A9 expression is seen in tumor-infiltrating cells in many epithelial tumors (reviewed in Refs. 6, 17). The proteins function predominantly as S100A8/A9 heterodimers and are chemotactic for leukocytes, thereby amplifying the local proinflammatory microenvironment. Similar to IL-1β, IL-6, and PGE_2, S100A8/A9 proteins mediate their effects by binding to plasma membrane receptors on their target cells. These receptors include heparan sulfate (18), TLR4 (19), and carboxylated N-glycans (20). Carboxylated N-glycans are constitutively expressed on endothelial cells, macrophages, and dendritic cells and are recognized by the mAbGB3.1 (21, 22). Carboxylated N-glycans on RAGE play an important role in HMGB1-RAGE-mediated signaling (23). Interaction of RAGE with S100A12 was the first described receptor-ligand model for an S100 protein (24). Although direct binding of S100A8/A9 to RAGE was not previously demonstrated, recent studies show that such interactions are likely (25, 26). In addition, we found that

*Department of Biological Sciences, University of Maryland Baltimore County, Baltimore, MD 21250; †Department of Pediatrics, University of Münster, Münster, Germany; and ‡Tumor Microenvironment Program, Cancer Center, The Burnham Institute for Medical Research, La Jolla, CA 92037

Received for publication May 7, 2008. Accepted for publication August 5, 2008.

The costs of publication of this article were defrayed in part by the payment of page charges. This article must therefore be hereby marked *advertisement* in accordance with 18 U.S.C. Section 1734 solely to indicate this fact.

[1] These studies were supported by National Institutes of Health Grants NIH R01CA84232 and NIH R01CA115880, Susan G. Komen Foundation BCTR0503885 (to S.O.R.), and NIH R01CA92608 (to H.F. and G.S.).

[2] Address correspondence and reprint requests to Dr. S. Ostrand-Rosenberg, Department of Biological Sciences, University of Maryland Baltimore County, 1000 Hilltop Circle, Baltimore, MD 21250. E-mail address: srosenbe@umbc.edu

[3] Abbreviations used in this paper: RAGE, receptor for advanced glycation end-product; MDSC, myeloid-derived suppressor cell; HA hemagglutinin; HG, housekeeping gene; CM, conditioned media; CAC, colitis-associated cancer; iNOS, inducible NO synthase.

S100A8/A9 bind to a subpopulation of RAGE modified by carboxylated glycans (27). A glycan-specific Ab, mAbGB3.1, blocks the onset of inflammation and reverses its early stage progression in a T cell model of colitis (22), a model in which RAGE and S100A8/A9 are up-regulated in colon and secondary lymphoid organs. The Ab also reduces the incidence of colitis-associated colon cancer (CAC) (27).

Because S100A8/A9 proteins are elevated in inflammation and cancer and are chemotactic, we hypothesized that they may contribute to the recruitment and retention of MDSC. We report here that MDSC from tumor-bearing mice not only have receptors for S100A8/A9, but also synthesize and secrete these proteins, providing an autocrine pathway for MDSC accumulation. Treatment of tumor-bearing mice with the mAbGB3.1, which binds to carboxylated N-glycans on cell surface receptors, blocks S100A8/A9 binding and signaling, reduces serum levels of S100A8/A9, and reduces the accumulation of MDSC in the blood and secondary lymphoid organs. Therefore, S100A8/A9 proteins are another class of proinflammatory mediators that complicate cancer immunotherapy strategies by promoting the accumulation of MDSC that block tumor immunity.

Materials and Methods

Mice

BALB/c and transgenic DO11.10 (I-A^d-restricted, OVA peptide 323–339-specific) (28) and clone 4 (H-$2K^d$-restricted, hemagglutinin (HA) peptide 518–526-specific) (28) mice were bred in the University of Maryland Baltimore County animal facility. All animal procedures were approved by the University of Maryland Baltimore County Institutional Animal Care and Use Committee.

Abs and flow cytometry

Fluorescently coupled Gr1, CD11b, IL-4Rα, CD80, arginase, inducible NO synthase (iNOS), Ly-6G, Ly-6C, and isotype control Abs were purchased from BD Pharmingen. F4/80 and Fc block Ab were purchased from Caltag Laboratories. S100A8 and S100A9 Abs were from Santa Cruz Biotechnology. Commercial Abs were used at a concentration of 4–10 μg/ml. mAbGB3.1 and isotype control Ab (21) were used at 40 μg/ml. Intracellular and cell surface staining were performed as described (28). Stained samples were run on a Beckman Coulter XL flow cytometer and analyzed using FCS-Express analysis software.

Tumor cells, tumor cell inoculation, tumor growth, surgery, and Ab treatment

4T1 mouse mammary carcinoma cells were maintained as described (29). For tumor progression experiments, BALB/c mice were inoculated in the abdominal mammary gland with 7000 4T1 cells, and tumor progression, surgical removal of primary tumors, and quantification of metastatic disease were performed as described (29). mAbGB3.1 or isotype control Ab treatment (10 μg protein/gm body weight, i.v.) was started 3 days after removal of primary tumor and continued once weekly. Seventy-two h after each treatment, mice were tail bled into 500 μl of a 0.008% heparin solution, and RBCs were removed by lysis (30). Remaining white cells were identified by flow cytometry (28). Ab treatment was terminated when mice were moribund and spleens, lymph nodes, and lungs were cryopreserved for immunohistochemistry.

MDSC purification, phenotype, morphology, and T cell suppression assay

Spleens, lungs, and femurs were obtained from 4T1 tumor-bearing mice on day 33 after inoculation of 7000 4T1 tumor cells. Femurs were flushed with excess PBS using a syringe fitted with a 27-g needle. Spleens and lungs were dissociated to single-cell suspensions as described (29). Splenocytes, bone marrow, and lung cells were depleted of RBCs, and MDSC were isolated by magnetic bead sorting of $Gr1^+$cells using Miltenyi Biotec magenetic beads, as described (28). For blood MDSC, tumor-bearing mice were bled into 500 μl of a 0.008% heparin solution, and RBC removed by lysis as described (28). Remaining white blood cells that were >90% $Gr1^+CD11b^+$ were used in experiments. MDSC were phenotyped using fluorescent-conjugated Abs and stained with Wright-Giemsa stain using Diff-Quik (Dade Behring) (28). T cell suppression was assessed by coculturing DO11.10 or clone 4 splenocytes with irradiated-blood MDSC or MACS-purified MDSC and specific peptide as described (28).

Real-time RT-PCR analysis

MDSC from tumor-bearing mice were isolated as described. To obtain sufficient $Gr1^+CD11b^+$ cells from tumor-free mice, mice were bled as described and $Gr1^+CD11b^+$ cells were purified using Gr1 Ab and Miltenyi Biotec magnetic beads (28). The resulting cells were washed once with PBS, and the pellets were frozen in dry ice and sent to SuperArray (http://www.superarray.com/) for RT-PCR analysis. Results are expressed as the number of threshold cycles (Ct) needed to detect product, or the fold change of tumor MDSC vs naive MDSC as calculated by the $\Delta\Delta$Ct method (31) using the following formulas:

ΔCt = average Ct (experimental) − average Ct (housekeeping genes).
Fold change = 2^ (tumor MDSC ΔCt − naive MDSC ΔCt).

The HG panel included glucuronidase β, Hprt1, Hsp90ab1, Gapdh, and actin β cytoplasmic.

Immunohistochemistry

Cryosections (6 μm) were air-dried, fixed in cold acetone for 2 min at room temperature, rehydrated in PBS, stained with anti-mouse Abs to CD11b and Gr-1 (BD Pharmingen), followed by Alexa 594- or Alexa 488-conjugated secondary Abs (Invitrogen), cover-slipped with VectaShield DAPI mounting medium (Vector Laboratories), and examined using an inverted TE300 Nikon wide field fluorescence microscope and photographed with a CCD SPOT RT Camera (Diagnostic Instruments). Cells in three high power fields were counted for quantitation.

Western blots

Western blots were performed on 12% SDS-PAGE gels using equivalent amounts of cell lysate proteins of MACS-purified MDSC. Ten percent skimmed milk was used for blocking. S100A8 and S100A9 were detected with goat polyclonal abs (R&D Systems). RAGE and HMGB1 were detected using rabbit polyclonal anti-RAGE (22) and anti-HMGB-1 (Abcam), respectively, and bands were visualized using corresponding alkaline phosphatase-conjugated secondary Abs (Jackson ImmunoResearch Laboratories) followed by BCIP/NBT substrate (Sigma-Aldrich).

S100A8 and S100A9 quantification

Secreted S100A8 and S100A9 proteins were quantified by ELISA as described (32) with the following modifications: coating Ab was goat anti-mouse S100A9 mAb (R&D Systems). Culture supernatants of MDSC (30) or 4T1 tumor or serum from tumor-bearing mice were diluted in HBSS containing 0.05% Tween 20. Polyclonal rabbit anti-mouse S100A8 Ab (33) was biotinylated using normal human serum-biotin as per the manufacturer's protocol (Pierce) and used at a dilution of 1/1000. Incubation with biotinylated anti-S100A8 Ab was for 2 h at room temperature, followed by streptavidin alkaline phosphatase (Promega; 1/2000) for 1 h at room temperature. Wells were developed with *p*-nitrophenyl phosphate substrate and read at 405 nm. Purified S100A8/A9 (34) served as standard.

S100A8/A9 protein binding

Cell membranes were generated from 10^8 blood MDSC by homogenization in 10 mM Tris-HCl (pH 7.4), containing 200 mM sucrose and protease inhibitors (mixture of EDTA-free serine and cysteine protease inhibitors; Roche). Nuclei and cell debris were removed by centrifugation at 900 × *g* for 10 min at 4°C. Resulting supernatants were ultracentrifuged at 110,000 × *g* for 75 min at 4°C, and pellets resuspended in 200 μl of 10 mM Tris-HCl (pH 7.4) with 150 mM NaCl and protease inhibitors. Endogenous S100A8/A9 proteins were stripped by incubation in 50 mM glycine and 100 mM NaCl (pH 3.0) for 3 min at 4°C followed by neutralization with cold HBSS. Membranes were incubated with increasing concentrations of Na^{125}I-labeled purified S100A8/A9 (labeled using Iodobeads (Pierce) as per the manufacturer's protocol to a specific activity of 2×10^5 cpm/pmol) for 1 h at 4°C in HBSS, washed twice with 1 ml of HBSS, recovered by ultracentrifugation, solubilized in 0.2 ml of 0.5 M NaOH, and cell-bound radioactivity was counted. Nonspecific binding was determined by binding in the presence of 100-fold molar excess of cold ligand. Where required, binding was conducted in the presence of 10-fold molar excess of mAbGB3.1, anti-RAGE, anti-S100A8, or isotype-matched irrelevant mAb. Saturation binding kinetic analyses were performed using GraphPad Prism. Values were normalized for number of cells.

NF-κB phosphorylation

Blood MDSC (10^8/ml) were cultured with S100A8/A9 (5 μg/ml) or TNF-α (20 ng/ml), with or without mAb GB3.1 or control irrelevant mAb (10 μg/ml) in 250 μl of serum-free DMEM in 24-well plates. At the indicated times,

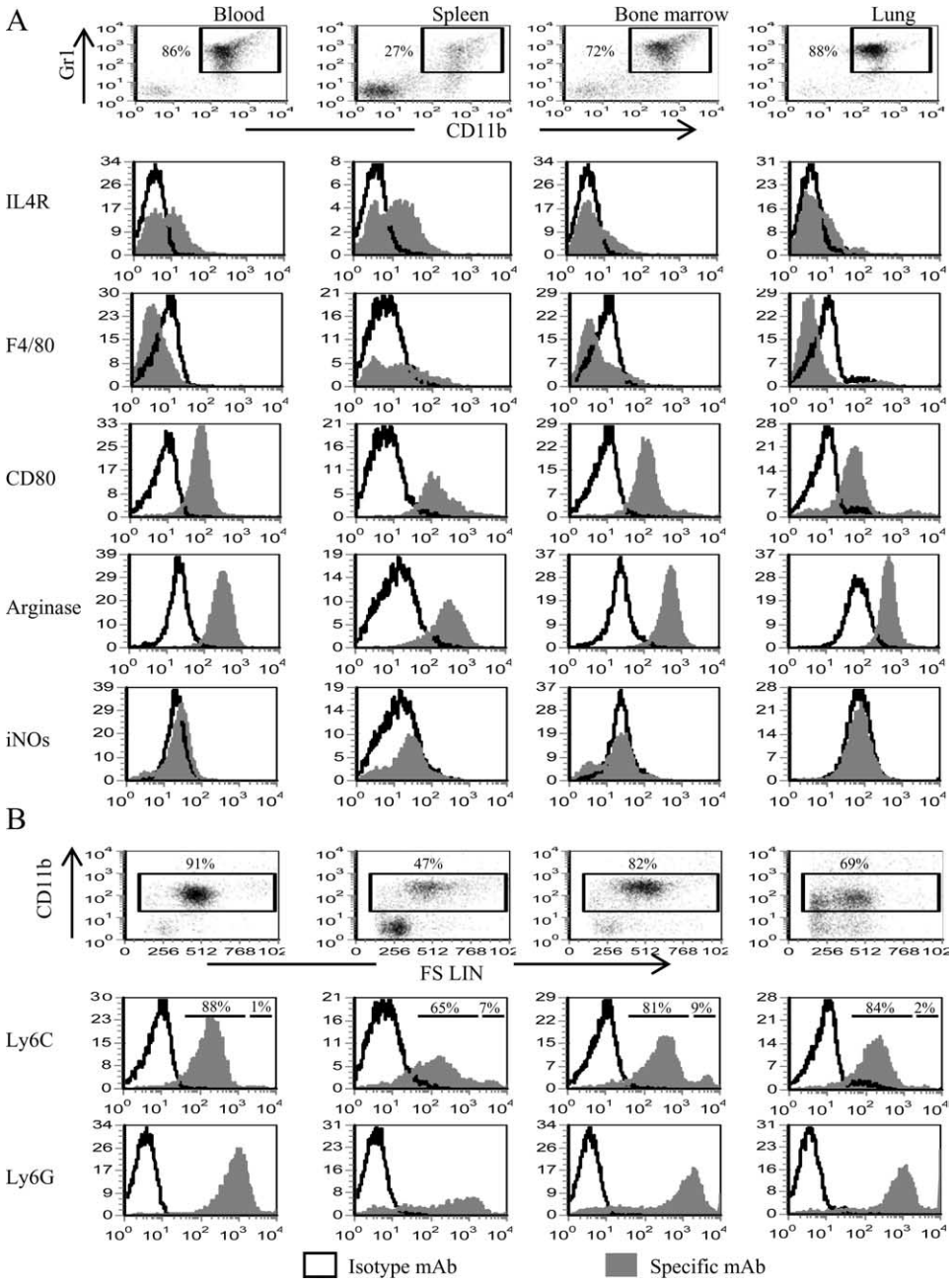

FIGURE 1. MDSC present in the bone marrow, blood, spleen, or lungs of BALB/c mice with the 4T1 mammary carcinoma are $Gr1^{high}CD11b^{high}$ $F4/80^{-}$IL-$4R\alpha^{+/-}CD80^{+}Arginase^{+}$ and have a mixed nuclear phenotype. *A*, Spleens, blood, bone marrow, and metastatic lung from BALB/c mice with 33-day primary tumors (11.5 mm in diameter) were harvested and the cells were stained with Abs to Gr1, CD11b, F4/80, IL-4Rα, CD80, arginase, iNOS, Ly-6C, and Ly-6G. $Gr1^{+}CD11b^{+}$ populations were gated and further analyzed by flow cytometry for F4/80, IL-4Rα, CD80, arginase, or iNOS. *B*, $CD11b^{+}$ cells of *A* were gated and analyzed for Ly6G and Ly6C. *C*, Cell populations from *A* were stained with Diff-Quik and analyzed by microscopy. Each panel shows representative cells assembled from three to six fields per MDSC sample. *D*, Purified $Gr1^{+}CD11b^{+}$ cells from the spleen, bone marrow, blood, or metastatic lungs were cocultured with transgenic $CD4^{+}$ D011.10 or $CD8^{+}$ Clone 4 splenocytes plus $OVA_{323-339}$ or $HA_{518-526}$ peptides, respectively, and T cell activation measured by tritiated thymidine uptake.

MDSC were washed with cold PBS and lysed in 200 μl lysis buffer (Cell Signaling Technology) containing PMSF (1 mM) and protease inhibitors (1 tab/10 ml lysis buffer). Cell lysates were centrifuged at 4°C and supernatants stored at −80°C until analyzed by PathScan Inflammation MultiTarget Sandwich ELISA Kit or PathScan phospho-NF-κB p65 (Ser536) Sandwich ELISA Kit according to the manufacturer's protocol (Cell Signaling Technology). Percentage increase in pNF-κB = (100%) × [(MDSC with inducer) − (MDSC without inducer)/(MDSC without inducer)].

Chemotaxis

In vitro migration of MDSC was evaluated in 24-well plates with transwell polycarbonate permeable supports (8.0 μm) (Costar Corning). One million MDSC (>90% $Gr1^{+}CD11b^{+}$ cells) were plated in 100 μl of serum-free IMDM in the upper compartment and 500 μl of chemoattractant (tumor-conditioned media (CM) ± 10 μg of Abs to S100A8 or S100A9, or IgG control Ab) were added to the lower compartment. Plates were incubated at 37°C with 5% CO_2 for 3 h, and the number of MDSC in the bottom compartment counted. For CM, supernatants were harvested from confluent cultures of 4T1 tumor cells cultured in medium IMDM containing 3% serum and 1% antibiotics. CM was filter sterilized and stored at −80°C as single-use aliquots. Percentage increase in migration of $Gr1^{+}CD11b^{+}$ cells = (100%) × [(MDSC migration with inducer ± Ab) − (MDSC migration in media control)/(MDSC migration in media control)].

Statistical analysis

Student's two-tailed *t* test was performed using Microsoft Excel 2000.

Results

MDSC in the blood, spleen, and bone marrow of 4T1 tumor-bearing mice, and metastatic 4T1 tumors, have a similar phenotype and suppressive activity

MDSC accumulate at the site of tumor and are elevated in the blood, bone marrow, and spleens of tumor-bearing mice. To confirm that MDSC within a given individual are homogeneous regardless of location, splenocytes, circulating leukocytes (blood), bone marrow cells, and lungs containing metastases were isolated from BALB/c mice that had been inoculated in the mammary fat pad 33 days earlier with 7000 4T1 tumor cells. The resulting cells were analyzed by immunofluorescence and flow cytometry for the

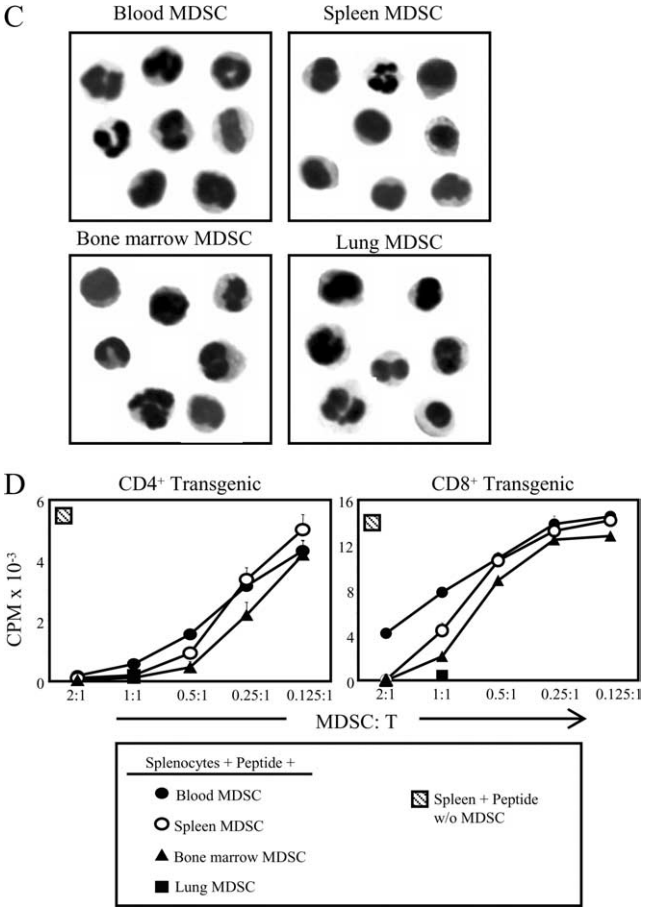

FIGURE 1. (*continued*)

canonical MDSC markers Gr1 and CD11b, and gated $Gr1^+CD11b^+$ cells were further analyzed for F4/80, IL-4Rα, and CD80, markers that are differentially expressed on MDSC isolated from mice with histologically distinct tumors (35, 36). The percentage of $Gr1^+CD11b^+$ cells differed in each tissue; however, $Gr1^+CD11b^+$ cells from all locations shared a similar phenotype ($Gr1^{high}CD11b^{high}F4/80^-CD80^+IL\text{-}4Ra^{+/-}Arginase^+$) (Fig. 1*A*). Previous studies have classified $Gr1^+CD11b^+$ cells as either "neutrophil-like" or "monocyte-like" based on the expression of Ly6G (immature neutrophil marker) or Ly6C (monocyte/macrophage marker), respectively, and nuclear morphology (35, 37–39). To determine whether differentially localized $Gr1^+CD11b^+$ cells are distinguished by either of these categories, $CD11b^+$ cells were gated and analyzed for Ly6G and Ly6C (Fig. 1), and $Gr1^+CD11b^+$ cells were Wright-Giemsa stained and examined histologically (Fig. 1*C*). All MDSC express Ly6C and Ly6G, although MDSC from bone marrow and spleen of 4T1 tumor-bearing mice have small subpopulations (9 and 7%, respectively) of $Ly6C^{high}$ cells. As previously reported for blood MDSC (30), 4T1-induced $Gr1^+CD11b^+$ cells from all locations are a mixture of cells with single- and multilobed nuclei (Fig. 1*C*). To confirm that MDSC are consistently suppressive regardless of their location, MDSC from blood, spleen, bone marrow, and lung (all $\geq$ 85% $Gr1^+CD11b^+$) were cocultured at varying ratios with splenocytes from transgenic D011.10 ($CD4^+$) or Clone 4 ($CD8^+$) mice and their respective peptides, and T cell proliferation was measured by uptake of [^{3}H]thymidine (Fig. 1*D*). These results combined with previous studies demonstrating that splenic MDSC from tumor-free mice are equally suppressive on a per cell basis as splenic MDSC from tumor-bearing mice (28), demonstrate that MDSC

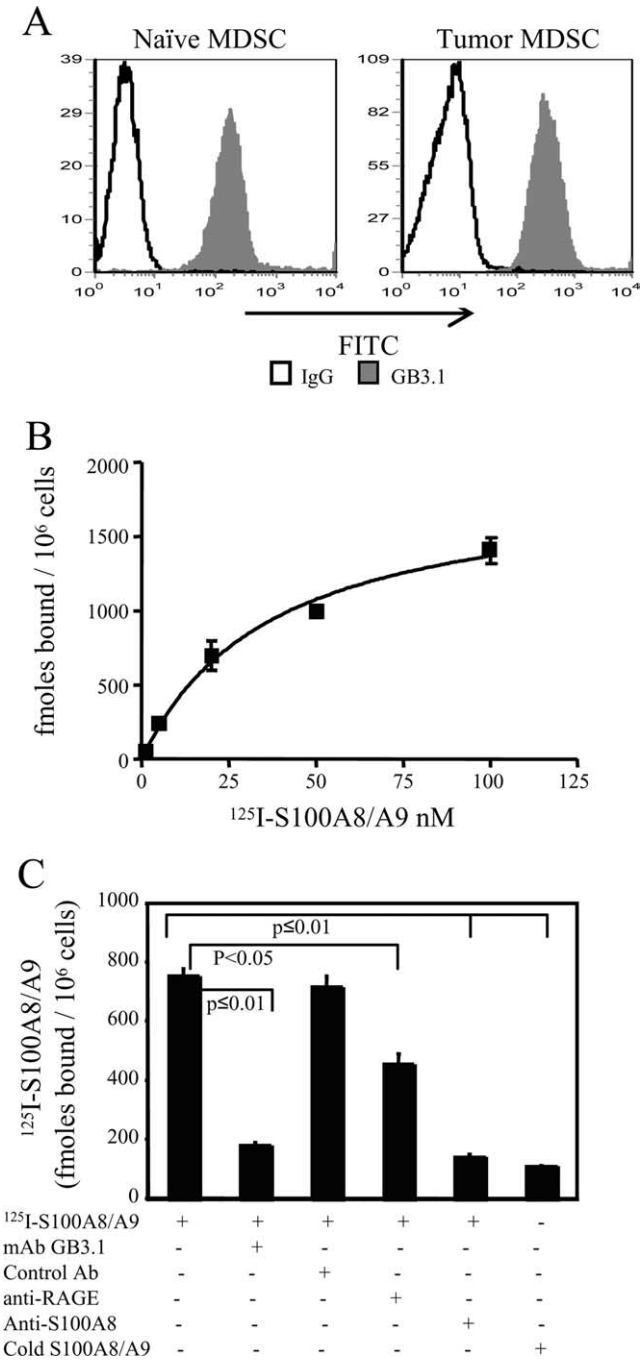

FIGURE 2. MDSC have glycoprotein receptors for and bind S100A8/A9 proteins. *A*, Leukocytes from the blood of tumor-free or 4T1 tumor-bearing BALB/c mice were stained with Gr1, CD11b, and GB3.1 mAbs. $Gr1^+CD11b^+$ cells were gated and analyzed for expression of GB3.1 receptors. *B*, Cell membranes of MDSC derived from 4T1 tumor-bearing mice were incubated with increasing concentrations of ^{125}I-S100A8/A9 proteins for 1 h at 4°C followed by washing, and membrane bound radioactivity was measured. Saturation binding kinetic analysis was performed using GraphPad Prism. Values represent mean ± SD of two independent experiments. *C*, Inhibition of binding of ^{125}I-S100A8/A9 to MDSC. MDSC membranes were incubated with ^{125}I-S100A8/A9 proteins (20 nM) in the presence or absence of mAbGB3.1, anti-RAGE, anti-S100A8 (10-fold molar excess), cold ligand (100-fold molar excess), or isotype control Abs. Membrane-bound radioactivity was determined as in *A*. Data are from one of two independent experiments.

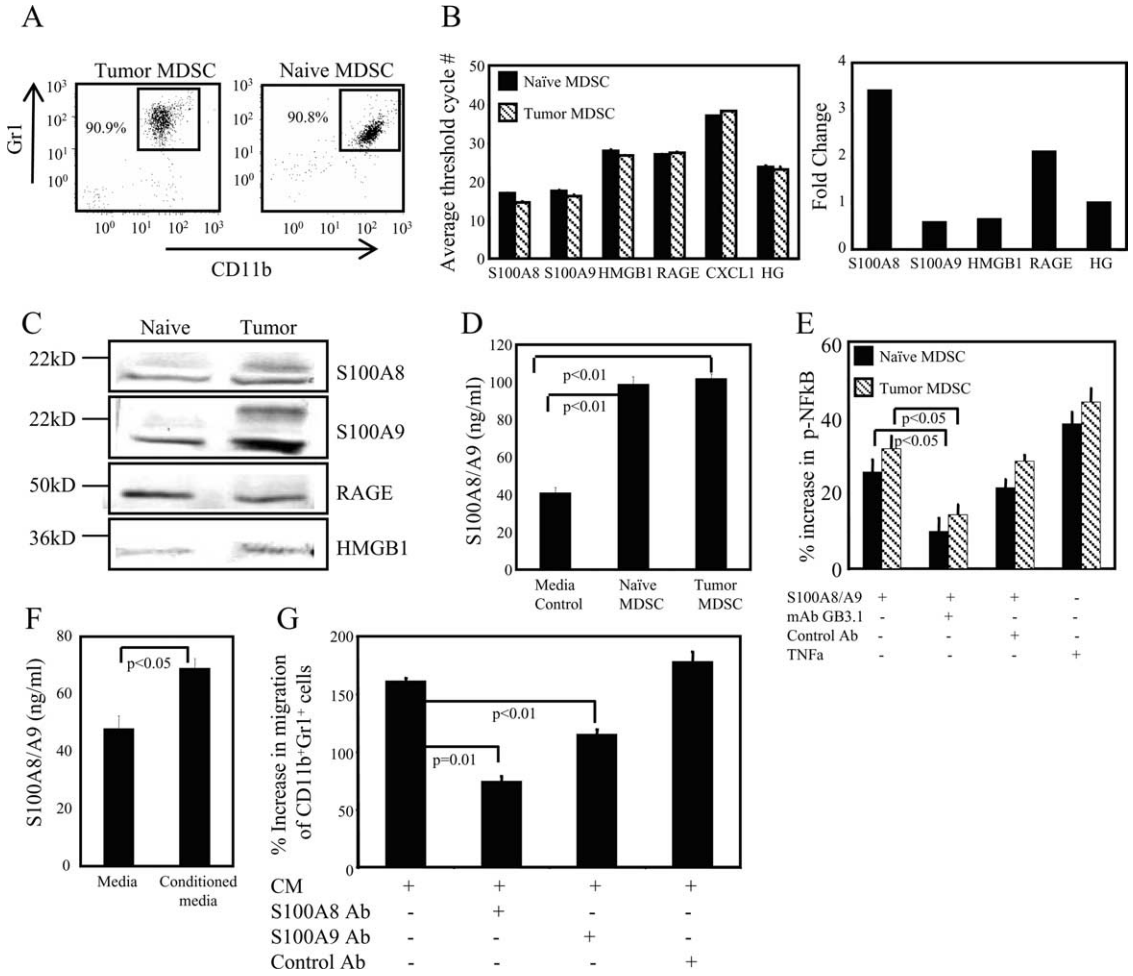

FIGURE 3. MSDC express and secrete S100A8/A9, and migrate and signal through NF-κB in response to S100A8/A9. *A*, Circulating white blood cells pooled from five 4T1 tumor-bearing mice (*left panel*) or pooled white blood cells purified by MACS sorting for Gr-1 from 60 tumor-free mice (*right panel*) were stained with fluorescent Abs to Gr1 and CD11b and analyzed by flow cytometry. *B*, MDSC contain elevated levels of mRNA for proinflammatory mediators. Real-time RT-PCR was performed on mRNA obtained from the purified cells of *A*. Expression levels are presented as the number of threshold cycles ± SD needed to detect a product. Fold increase is the relative increase in MDSC from tumor-bearing mice vs tumor-free mice. Values for the HG are the average of five genes: GAPDH, Hprt1, Hsp90ab1, actin β cytoplasmic, and glucuronidase β. CXCL1 is included as an example of a poorly expressed gene. *C*, Lysates of the $Gr1^+CD11b^+$ cells shown in *A* were electrophoresed on 12% SDS-PAGE gels, and Western blotted with Abs to S100A8, S100A9, HMGB1, and RAGE. *D*, MDSC purified from BALB/c 4T1 tumor-bearing or from tumor-free mice were cultured for 16 h, and the supernatants were assayed by ELISA for S100A8/A9 proteins. Data are from one of two independent experiments. *E*, NF-κB is phosphorylated in MDSC following binding of S100A8/A9 proteins. MDSC from tumor-bearing or tumor-free mice were cocultured with S100A8/A9 or TNF-α for 10 min and cell lysates were screened for phosphorylated-NF-κB p65 (ser536) by ELISA. Data are from one of two independent experiments. *F*, CM from 4T1 tumor cells was tested by ELISA for S100A8/A9. *G*, 4T1 tumor cells secrete S100A8/A9 proteins that are chemotactic for MDSC. Blood MDSC (>90% $Gr1^+CD11b^+$ cells) were tested by chemotaxis assay for their migration in response to 4T1 CM. Data are pooled from two independent experiments.

from different anatomical locations have approximately equivalent suppressive activity. Therefore, anatomical location does not affect the phenotype or function of MDSC, and subsequent experiments performed with blood MDSC are representative of MDSC from all locations.

MDSC have receptors for the S100A8/A9 proinflammatory proteins

Several observations circumstantially link S100 proinflammatory proteins with MDSC. Inflammation is an inducer of MDSC (8, 10, 11). Proinflammatory S100 proteins are present in the tumor environment of mammary carcinomas (40, 41), and over-expression of S100A8/A9 heteromeric complexes is associated with poor prognosis in invasive ductal carcinoma of the breast (42). We therefore examined whether MDSC induced by the 4T1 mammary carcinoma express receptors for S100 proteins. Blood was collected from tumor-free mice and from BALB/c mice 31 days after 4T1 inoculation, when metastatic disease was established and primary tumors were 9.41 ± 0.3 mm in diameter. We found that $Gr1^+CD11b^+$ leukocytes from both tumor-free and tumor-bearing mice stained with mAbGB3.1, which detects carboxylated N-glycans expressed on cellular receptor(s) for S100A8/A9 proteins (20, 21) (Fig. 2*A*). In addition, cell membranes prepared from blood MDSC (>90% $Gr1^+CD11b^+$) had specific saturable binding sites for ^{125}I-S100A8/A9 with a K_d of 37.43 ± 6.99 nM and a Bmax of 1.882 ± 0.142 pmols/million cells (Fig. 2*B*). ^{125}I-S100A8/A9 binding was displaced by molar excess of cold ligand or by anti-S100A8 Abs (Fig. 2*C*). To ascertain that the S100A8/A9 heterodimers were binding to carboxylated N-glycans on cell surface receptors, MDSC membranes were incubated with ^{125}I-S100A8/A9 proteins in the presence of mAbGB3.1. Binding was significantly reduced in the presence of mAbGB3.1 (Fig. 2*C*), while an isotype control Ab had no effect on binding. Interestingly, anti-RAGE also partially blocked binding, consistent with our earlier reports that RAGE is modified by carboxylated N-glycans (23) and that

S100A8/A9 proteins bind to RAGE (27). Therefore, MDSC from tumor-free mice and from mice with primary and metastatic mammary carcinoma contain carboxylated N-glycan receptors that bind S100A8/A9, consistent with the concept that proinflammatory S100 proteins are part of the inflammatory milieu that induces the accumulation of MDSC.

MDSC synthesize and secrete S100A8/A9 heterodimers

Since S100A8/A9 proteins are synthesized by cells of the myeloid lineage, we reasoned that MDSC may also contribute to the inflammatory milieu by producing these proinflammatory mediators. To test this hypothesis, we bled mice on day 36 after 4T1 inoculation when $Gr1^+CD11b^+$ cells were >90% of the circulating white cells (Fig. 3*A*, *left panel*), primary tumors were 9.70 ± 0.21 mm in diameter, and metastatic disease was established. Tumor-free mice were also bled and $Gr1^+CD11b^+$ cells, comprising <10% of the circulating white cells, were purified to >90% purity (Fig. 3*A*, *right panel*). Real-time RT-PCR was performed and the number of cycles required to amplify these messages was compared with that required for a panel of five HG and the poorly expressed CXCL1 gene (Fig. 3*B*, *left panel*). $Gr1^+CD11b^+$ cells from both tumor-free and tumor-bearing mice expressed elevated levels of S100A8/A9 relative to the HG (Fig. 3*B*). RAGE and HMGB1 transcripts were also expressed; however, at somewhat lower levels than the HG. S100A8 and RAGE were increased 2- to 3-fold in $Gr1^+CD11b^+$ cells from tumor-bearing mice vs tumor-free mice (Fig. 3*B*, *right panel*).

To confirm the PCR results, lysates of the purified MDSC were analyzed by Western blotting for S100A8/A9, HMGB1, and RAGE (Fig. 3*C*). S100A8 and S100A9 monomers and low levels of HMGB1 were present in $Gr1^+CD11b^+$ cells from both tumor-bearing and tumor-free mice. HMGB1 levels in MDSC increase in the presence of tumor, and multimers of S100A8/A9, which are the active forms, were only present in MDSC from tumor-bearing mice. In contrast to mRNA levels, S100A9 protein level is greatly increased in tumor MDSC in relation to S100A8. This could be related to inefficient translation of S100A8 mRNA and/or stability of S100A8 protein (43, 44). Collectively, the PCR and protein data suggest that expression of S100A8 is S100A9-dependent and that S100A8 acquires stability by S100A8/A9 heterocomplex formation (42). In fact, S100A8/A9 heterodimer is extremely protease resistant relative to the homodimers (45). Therefore, MDSC from tumor-bearing mice, but not from tumor-free mice, contain functionally active S100A8/A9 proteins, consistent with the concept that these proinflammatory mediators and receptors of MDSC are regulated by tumor.

Upon cellular activation, S100A8/A9 are secreted into the extracellular milieu where they mediate leukocyte recruitment and other functions that promote inflammation (15). If MDSC contribute to the inflammatory milieu, then they may secrete S100A8/A9 proteins. To test this possibility, equal numbers of circulating white blood cells from BALB/c mice with advanced 4T1 tumors (>95% $Gr1^+CD11b^+$ cells) and purified MDSC from tumor-free mice (>95% $Gr1^+CD11b^+$) were cultured for 24 h and the supernatants assayed by ELISA for S100A8/A9 proteins. MDSC from both tumor-bearing and tumor-free mice released significant amounts of S100A8/A9 proteins on a per cell basis (Fig. 3*D*). Therefore, MDSC not only have the capacity to respond to S100A8/A9 proteins, but they may also sustain an autocrine stimulatory pathway by secreting active S100A8/A9 proteins.

S100A8/A9 signal through the NF-κB pathway in MDSC

To determine whether S100A8/A9 proteins activate MDSC after binding to cell surface receptors, we examined potential signaling

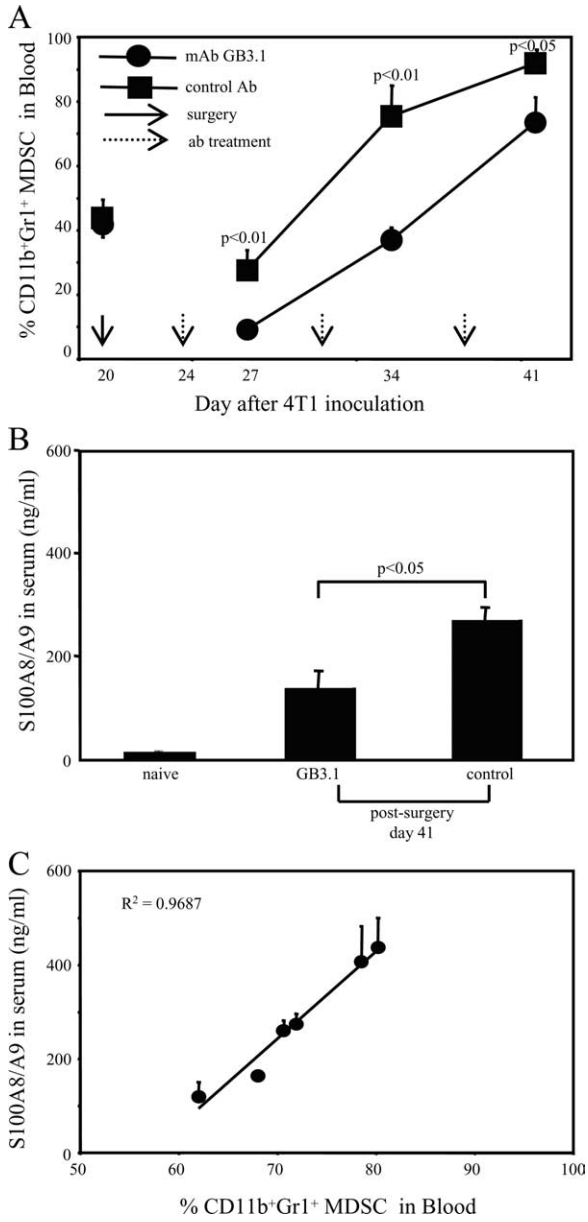

FIGURE 4. mAbGB3.1 reduces MDSC and S100A8/A9 proteins in the blood of tumor-bearing mice. *A*, mAbGB3.1 treatment reduces serum levels of MDSC in tumor-bearing mice. BALB/c mice were inoculated on day 0 with 4T1 tumor cells, their primary tumors were removed on day 20, and GB3.1 or control Ab treatment was started 3 days later (day 24) and continued once weekly. Mice were bled 72 h after each Ab treatment and their white blood cells stained for Gr1 and CD11b. At the time of surgery, primary tumor diameters were 5.09 ± 0.76 and 5.36 ± 0.68 mm, and percent $Gr1^+CD11b^+$ MDSC in the blood were 41.25 ± 3.98 and 44.65 ± 6.60%, for the mAbGB3.1 and control Ab-treated groups, respectively. Data are the average ± SD of four mice in each group. Experiment was terminated on day 42 when mice were moribund. Data are from one of two independent experiments. *B*, mAbGB3.1 treatment reduces serum levels of S100A8/A9 proteins. GB3.1 and control Ab-treated postsurgery mice from *A* were bled on day 41 (20 days after surgery), and the serum assayed by ELISA for S100A8/A9 proteins. Serum from tumor-free (naive) mice was included for comparison. *C*, Serum S100A8/A9 levels are proportional to the amount of circulating MDSC. Tumor-bearing mice were bled and serum levels of S100A8/A9 were determined by ELISA and the percent of MDSC determined by flow cytometry. Data are from one of two independent experiments.

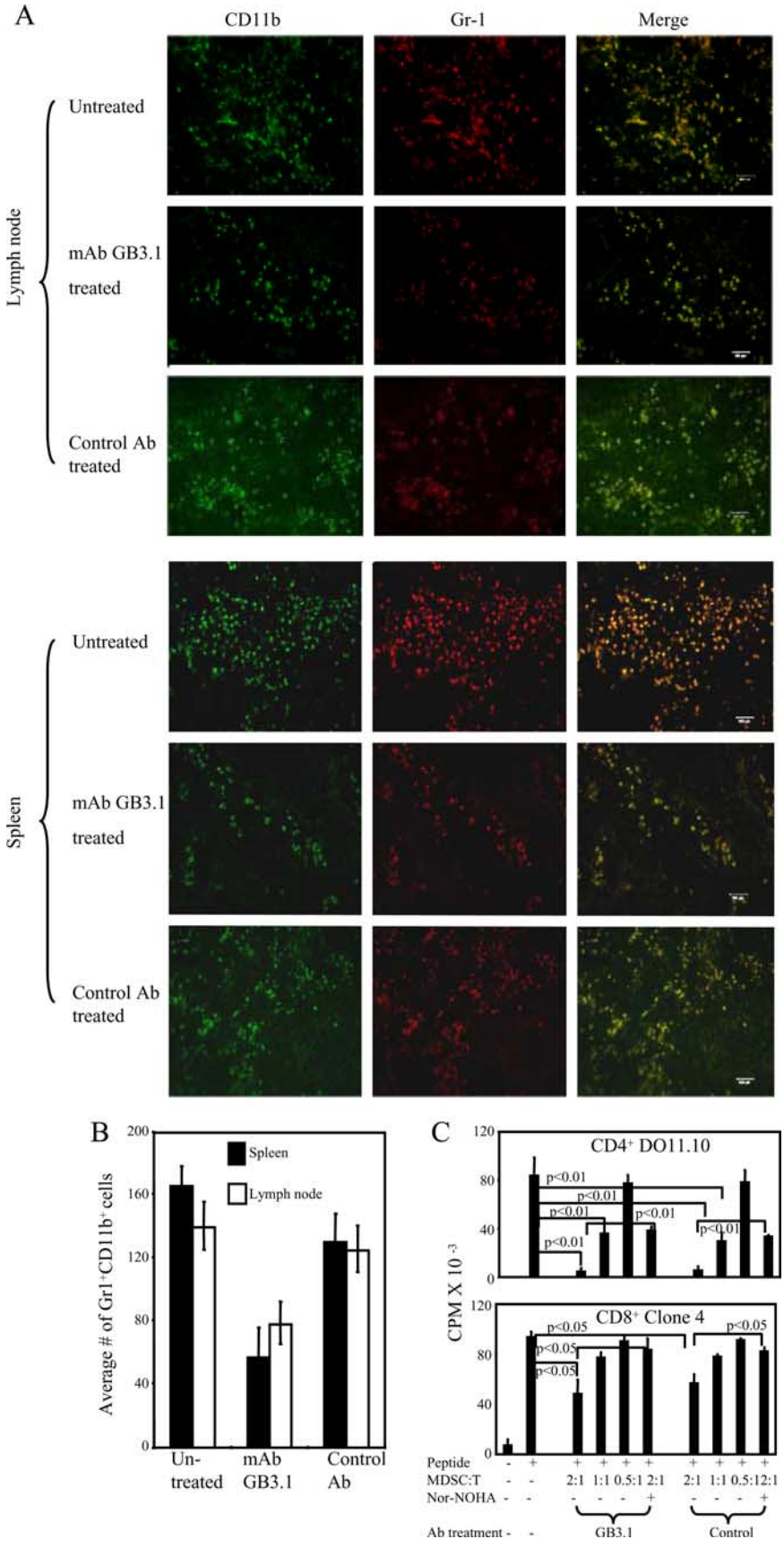

FIGURE 5. Blocking S100A8/A9 binding reduces MDSC accumulation in vivo in tumor-bearing mice but does not alter immunosuppressive activity of MDSC on a per cell basis. *A*, Spleen and lymph nodes from BALB/c mice with 41 day 4T1-tumors were cryo-preserved and stained for CD11b and Gr-1. Representative sections are shown. Scale bars indicate 100 microns. *B*, Average number of $Gr1^+CD11b^+$ cells counted in three high power fields of lymph nodes and spleen for untreated, mAb GB3.1-treated, and control Ab-treated groups. *C*, $CD4^+$ DO11.10 or $CD8^+$ Clone 4 transgenic splenocytes were cocultured with OVA or HA peptide, respectively, in the presence or absence of graded doses of MACS-sorted splenic $Gr1^+CD11b^+$ MDSC (>90% $Gr1^+CD11b^+$) from mAbGB3.1 or control mAb-treated postsurgery BALB/c mice. BALB/c mice were inoculated on day 0 with 4T1 cells, primary tumors were removed on day 26 (primary tumor diameters were 4.64 ± 0.55 and 5.33 ± 0.32 for control and mAbGB3.1 depletion groups, respectively), mAbGB3.1 or control Ab treatment was started on day 29, and MDSC were harvested 1 day after the last Ab treatment on day 45. T cell activation was measured by [^{3}H]thymidine incorporation. Data are from one of two independent experiments.

pathways in the $Gr1^+CD11b^+$ cells. Circulating white blood cells were obtained from BALB/c mice on day 31 after 4T1 inoculation (>95% $Gr1^+CD11b^+$ cells) and were purified from tumor-free mice (>95% $Gr1^+CD11b^+$), cocultured with endotoxin-free S100A8/A9 proteins, and cell lysates assayed by ELISA for phosphorylated NF-κB and MAPK pathway signaling molecules, two

pathways activated by inflammation. None of the molecules in the MAPK pathway were affected (data not shown). However, NF-κB was phosphorylated in MDSC from both tumor-bearing and tumor-free mice within the first 10 min of incubation at a level comparable to activation by TNF-α, a NF-κB-dependent gene that is known to be activated by S100A8/A9 (22) (Fig. 3*E*). S100A8/A9-induced activation was reduced in the presence of mAbGB3.1. Therefore, S100A8/A9 proteins activate the NF-κB pathway in MDSC, and this activation is mediated in part by binding to cell surface receptors expressing carboxylated glycans.

S100A8/A9 proteins are chemotactic for MDSC

In addition to myeloid cells and MDSC, S100A8/A9 proteins are produced by many tumor cells (40, 41, 46–49) and are chemotactic for target cells expressing their receptor (20, 50), raising the possibility that tumor cell and/or MDSC-secreted S100A8/A9 proteins attract MDSC to tumor sites. To test this concept, supernatants from 4T1 cultures were assayed for S100A8/A9 and MDSC were tested for migration in response to 4T1 supernatants, using transwell chambers. We found that 4T1 cells secrete S100A8/A9 proteins (Fig. 3*F*) and 4T1 supernatants are chemoattractants for MDSC (Fig. 3*G*). Chemotaxis was mediated by S100A8/A9 in the culture supernatants, since migration was reduced in the presence of Abs to S100A8 or S100A9.

Blocking of S100A8/A9 binding reduces the levels of MDSC and S100A8/A9 proteins in the blood of tumor-bearing mice

If S100A8/A9-mediated signaling promotes recruitment of MDSC, then inhibition of S100A8/A9 binding in vivo may reduce MDSC levels. To test this possibility, mAbGB3.1 or irrelevant control mAb was administered to BALB/c mice with established metastatic disease whose primary 4T1 tumors were surgically removed. This experimental design was used for two reasons: (i) we previously demonstrated that MDSC levels decrease with removal of primary tumor, and rapidly increase thereafter unless there is therapeutic intervention (30, 51). (ii) This setting closely models the conditions under which immunotherapy would be administered clinically and we wanted to see whether mAbGB3.1 could facilitate a reduction in MDSC in a clinically relevant situation. Mice were inoculated on day 0 with 4T1 tumor cells, primary tumors were surgically resected on day 20, and mAbGB3.1 or irrelevant isotype control Ab treatment was started on day 24. Primary tumor diameters (5.09 ± 0.76 and 5.36 ± 0.68 mm) and percent MDSC in blood (41.25% ± 3.98 and 44.65% ± 6.60) were matched at the time of surgery for mAbGB3.1 and control Ab treated groups, respectively. Mice were bled 3 days after each Ab treatment, and their circulating white blood cells were stained for Gr1 and CD11b. Consistent with previous observations, removal of primary tumor temporarily reduced MDSC levels in the blood (28). Treatment with mAbGB3.1 significantly decreased the accumulation of MDSC relative to treatment with control mAb (Fig. 4*A*), and did not affect the levels of other peripheral blood monocytes, dendritic cells, T cells, or B cells (data not shown).

If MDSC production of S100A8/A9 proteins contributes to the overall inflammatory milieu in tumor-bearing individuals, then these proteins should be elevated in tumor-bearing mice and reduction of MDSC should result in a concomitant decrease in serum S100A8/A9. To test this hypothesis, we measured the levels of S100A8/A9 proteins in the serum of tumor-free and tumor-bearing mice treated with mAbGB3.1 or control mAb. Treatment with mAbGB3.1 significantly reduced serum levels of S100A8/A9 in tumor-bearing mice (Fig. 4*B*), and the level of serum S100A8/A9 in tumor-bearing mice was roughly proportional to the quantity of MDSC in the blood (Fig. 4*C*). mAbGB3.1 treatment did not affect the amount of S100A8/A9 released per cell in culture (not shown). Therefore, the accumulation of S100A8/A9 in the serum of tumor-bearing mice may be at least partially due to the production of these molecules by MDSC.

In vivo treatment with mAbGB3.1 reduces the accumulation of MDSC

In addition to accumulating in the blood, spleen, bone marrow, and tumor sites, MDSC are also found in the lymph nodes of tumor-bearing mice (52). To determine whether blockade of S100A8/A9 receptors reduces MDSC levels in sites other than the blood, BALB/c mice were inoculated with 4T1, primary tumor was surgically resected on day 20, and mAbGB3.1 or control Ab treatment was started on day 24. Secondary lymphoid organs and metastatic lungs were cryo-preserved on day 41, when mice had established primary tumors and metastatic disease, and were stained for $Gr1^+CD11b^+$ cells. $Gr1^+CD11b^+$ cells were present in high numbers in the lymph nodes and spleens of untreated mice, and mAbGB3.1 treatment reduced accumulation of these cells at these sites (Fig. 5, *A* and *B*) but not in the lungs (data not shown).

In addition to increasing the numbers of MDSC, S100A8/A9 proteins may increase MDSC suppressive activity. In this case, MDSC of tumor-bearing mice treated with mAbGB3.1 might be less suppressive on a per cell basis than MDSC of control Ab-treated mice. To test this hypothesis, mice were inoculated on day 0 with 4T1 cells, primary tumors were removed on day 26, mAbGB3.1 or control Ab treatment was started on day 29, and splenic MDSC were harvested, purified (>90% $Gr1^+CD11b^+$), and tested for their ability to suppress peptide-activation of $CD4^+$ DO11.10 or $CD8^+$ Clone 4 transgenic T cells (Fig. 5*C*). $Gr1^+CD11b^+$ MDSC from mAbGB3.1-treated and from control-treated mice were equally suppressive on a per cell basis, and both MDSC cell populations used arginase to mediate their suppressive effects, as shown by restoration of T cell proliferation in the presence of the arginase inhibitor, N^w-hydroxy-nor-$_L$-arginine diacetate salt. Therefore, S100A8/A9 proteins promote immune suppression by enhancing the recruitment and accumulation of $Gr1^+CD11b^+$ cells, but do not alter the suppressive activity of individual MDSC.

Discussion

Myeloid cells with potent immune suppressive activity are present in most patients and mice with malignant tumors and have stimulated considerable interest as potential targets for therapy. In mice they are commonly characterized by expression of the cell surface markers CD11b and Gr1, which are characteristic of monocytes/macrophages and granulocytes, respectively. These so-called "MDSCs" (53) have also been associated with other cell surface markers such as IL-4Rα (35, 54), F4/80 (35, 37, 55), CD80 (56), Ly6C, and Ly6G (37). However, none of these markers is definitive since their expression varies based on the inducing tumor. In addition to cell surface markers, MDSC have been characterized by their content of suppressive molecules including arginase (10, 57, 58), iNOS (59), and other reactive oxygen species (58, 60), and have been classified as "neutrophil-like" or "monocyte-like" based on their nuclear morphology (38). Since MDSC are induced by multiple tumor and/or host cell-secreted factors (61, 62), it is likely that the MDSC phenotypes reported in different tumor systems are due to different combinations of factors produced by different tumors. Therefore, aside from the markers Gr1 and CD11b and the ability to suppress T cell activation, there is no unique or combination of phenotypic markers that unambiguously identifies mouse MDSC. In contrast to MDSC induced by different tumors, MDSC at different sites within an individual are homogeneous in their

expression of phenotypic markers and they have the same suppressive activity, indicating that tissue localization does not alter MDSC phenotype or function. MDSC from 4T1 tumor-bearing mice have a consistent phenotype of $Gr1^+CD11b^+F4/80^-IL\text{-}4R\alpha^{+/-}Arginase^+iNOS^-CD80^+$, contradicting some studies suggesting that IL-4Rα is a definitive marker for mouse MDSC (35, 54). Because blood MDSC are easily obtainable in high purity and MDSC localized to different sites do not differ, in our studies, we have used blood MDSC as a prototype and demonstrate here that MDSC from naive and tumor-bearing mice also express carboxylated glycans, RAGE, S100A8/A9, and HMGB1, and respond to S100A8/A9.

Although the proinflammatory S100A8/A9 proteins are up-regulated in many cancer patients and they have been proposed as prognostic markers (42, 63), a role for these molecules in tumor promotion and progression has not previously been demonstrated. The present study was based on the hypothesis that S100A8/A9 proteins contribute to tumor growth by inducing MDSC, which block tumor immunity and thereby facilitate tumor progression. We now report that S100A8/A9 not only induce the accumulation of MDSC, but they are also secreted by MDSC and by tumor cells, and bind to cell surface receptors leading to signaling within MDSC and MDSC migration. Thus, the S100A8/A9 proteins provide for a positive autocrine feedback loop that ensures the maintenance of functionally suppressive MDSC within an inflammatory tumor environment. We recently showed that MDSC expressing S100A8/A9 accumulate in all regions of dysplasia and adenoma in a CAC model (27), and that $RAGE^{-/-}$ mice are resistant to the onset of CAC. Up-regulation of S100A8/A9 in various tumors (17), their positive autocrine secretion, and promotion of a feed forward loop involving receptors such as RAGE suggest that these proteins play an important role in inflammation mediated cancer progression.

As reported earlier, $Gr1^+CD11b^+$ MDSC from tumor-free mice and from mice with 4T1 tumors are equally suppressive on a per cell basis (28). This observation combined with the current findings that MDSC from both sources share a common phenotype and are both activated by S100A8/A9 through NF-κB supports the concept that tumors regulate the expansion of a normal myeloid cell population rather than induce a novel myeloid population. Indeed, multiple proinflammatory mediators including S100A8/A9 (this report), IL-1β (8, 11), IL-6 (9), and PGE_2 (10, 12) up-regulate MDSC, indicating that inflammation is an important contributing factor to the accumulation of MDSC in tumor-bearing individuals.

Our in vitro studies show that S100A8/9 binding to MDSC is dependent on carboxylated N-glycans and this binding is inhibited by mAbGB3.1, an Ab that recognizes carboxylated N-glycans. Carboxylated glycans are expressed on RAGE (23) and S100A8/A9 binds to a subpopulation of RAGE enriched for carboxylated glycans (27). The observation that inflammation-induced skin tumors in RAGE knockout mice have reduced levels of infiltrating MDSC also implicates RAGE in MDSC recruitment (6). Carboxylated glycans also bind Annexin I, S100A12, and HMGB1 (20, 23). Annexin I is anti-inflammatory. S100A12 and HMGB1 are ligands for RAGE, and our studies show that the binding of both ligands to RAGE is mediated by carboxylated glycans (20) (G. Srikrishna and H. Freeze, unpublished data). The role of S100A12 in our model is irrelevant since mice do not express S100A12 (64). However, the role of HMGB1 in mAbGB3.1-mediated effects on MDSC accumulation cannot be ruled out. Regardless of the nature and multiplicity of receptors and ligands, carboxylated glycan-mediated signaling in MDSC appears to converge with the activation of NF-κB.

In addition to S100A8/A9 proteins, MDSC are induced by other proinflammatory factors. Therefore, it is not surprising that in vivo blocking of S100A8/A9 binding reduces, but does not eliminate, MDSC accumulation in tumor-bearing mice. Since MDSC are a significant impediment to active T and NK cell immunotherapies (65), targeting of S100A8/A9 binding may improve immunotherapy with cancer vaccines and other immune strategies that require an immune-competent host. However, it is not clear what level of MDSC can be tolerated and still achieve active immunity, so optimal immunotherapy may require blocking or neutralizing all MDSC inducers. Interestingly, other proinflammatory mediators that activate MDSC also signal through the NF-κB pathway (S. Bunt, P. Sinha, V. Clements, and S. Ostrand-Rosenberg, unpublished observations), so drugs that target the NF-κB pathway may be particularly effective in reducing this tumor-promoting cell population.

Acknowledgments

We appreciate the technical support by Virginia K. Clements, the animal care by Terry King, the histology assistance of Robbin Newlin, and the illustrative contributions of Tim Ford. We thank Dr. Thomas Vogl, University of Münster, for the gift of S100A8/A9.

Disclosures

The authors have no financial conflict of interest.

References

1. Balkwill, F., and A. Mantovani. 2001. Inflammation and cancer: back to Virchow? *Lancet* 357: 539–545.
2. Coussens, L. M., and Z. Werb. 2002. Inflammation and cancer. *Nature* 420: 860–867.
3. Ruegg, C. 2006. Leukocytes, inflammation, and angiogenesis in cancer: fatal attractions. *J. Leukocyte Biol.* 80: 682–684.
4. Luo, J. L., S. Maeda, L. C. Hsu, H. Yagita, and M. Karin. 2004. Inhibition of NF-κB in cancer cells converts inflammation- induced tumor growth mediated by TNFα to TRAIL-mediated tumor regression. *Cancer Cell.* 6: 297–305.
5. Karin, M., and F. R. Greten. 2005. NF-κB: linking inflammation and immunity to cancer development and progression. *Nat. Rev. Immunol.* 5: 749–759.
6. Gebhardt, C., A. Riehl, M. Durchdewald, J. Nemeth, G. Furstenberger, K. Muller-Decker, A. Enk, B. Arnold, A. Bierhaus, P. P. Nawroth, et al. 2008. RAGE signaling sustains inflammation and promotes tumor development. *J. Exp. Med.* 205: 275–285.
7. Lin, W. W., and M. Karin. 2007. A cytokine-mediated link between innate immunity, inflammation, and cancer. *J. Clin. Invest.* 117: 1175–1183.
8. Bunt, S. K., P. Sinha, V. K. Clements, J. Leips, and S. Ostrand-Rosenberg. 2006. Inflammation induces myeloid-derived suppressor cells that facilitate tumor progression. *J. Immunol.* 176: 284–290.
9. Bunt, S. K., L. Yang, P. Sinha, V. K. Clements, J. Leips, and S. Ostrand-Rosenberg. 2007. Reduced inflammation in the tumor microenvironment delays the accumulation of myeloid-derived suppressor cells and limits tumor progression. *Cancer Res.* 67: 10019–10026.
10. Sinha, P., V. K. Clements, A. M. Fulton, and S. Ostrand-Rosenberg. 2007. Prostaglandin E_2 promotes tumor progression by inducing myeloid-derived suppressor cells. *Cancer Res.* 67: 4507–4513.
11. Song, X., Y. Krelin, T. Dvorkin, O. Bjorkdahl, S. Segal, C. A. Dinarello, E. Voronov, and R. N. Apte. 2005. $CD11b^+/Gr\text{-}1^+$ immature myeloid cells mediate suppression of T cells in mice bearing tumors of IL-1β-secreting cells. *J. Immunol.* 175: 8200–8208.
12. Rodriguez, P. C., C. P. Hernandez, D. Quiceno, S. M. Dubinett, J. Zabaleta, J. B. Ochoa, J. Gilbert, and A. C. Ochoa. 2005. Arginase I in myeloid suppressor cells is induced by COX-2 in lung carcinoma. *J. Exp. Med.* 202: 931–939.
13. Foell, D., H. Wittkowski, T. Vogl, and J. Roth. 2007. S100 proteins expressed in phagocytes: a novel group of damage-associated molecular pattern molecules. *J. Leukocyte Biol.* 81: 28–37.
14. Donato, R. 2001. S100: a multigenic family of calcium-modulated proteins of the EF-hand type with intracellular and extracellular functional roles. *Int. J. Biochem. Cell. Biol.* 33: 637–668.
15. Roth, J., T. Vogl, C. Sorg, and C. Sunderkotter. 2003. Phagocyte-specific S100 proteins: a novel group of proinflammatory molecules. *Trends Immunol.* 24: 155–158.
16. Foell, D., M. Frosch, C. Sorg, and J. Roth. 2004. Phagocyte-specific calcium-binding S100 proteins as clinical laboratory markers of inflammation. *Clin. Chim. Acta* 344: 37–51.
17. Gebhardt, C., J. Nemeth, P. Angel, and J. Hess. 2006. S100A8 and S100A9 in inflammation and cancer. *Biochem. Pharmacol.* 72: 1622–1631.
18. Robinson, M. J., P. Tessier, R. Poulsom, and N. Hogg. 2002. The S100 family heterodimer, MRP-8/14, binds with high affinity to heparin and heparan sulfate glycosaminoglycans on endothelial cells. *J. Biol. Chem.* 277: 3658–3665.

19. Vogl, T., K. Tenbrock, S. Ludwig, N. Leukert, C. Ehrhardt, M. A. van Zoelen, W. Nacken, D. Foell, T. van der Poll, C. Sorg, and J. Roth. 2007. Mrp8 and Mrp14 are endogenous activators of Toll-like receptor 4, promoting lethal, endotoxin-induced shock. *Nat. Med.* 13: 1042–1049.
20. Srikrishna, G., K. Panneerselvam, V. Westphal, V. Abraham, A. Varki, and H. H. Freeze. 2001. Two proteins modulating transendothelial migration of leukocytes recognize novel carboxylated glycans on endothelial cells. *J. Immunol.* 166: 4678–4688.
21. Srikrishna, G., D. K. Toomre, A. Manzi, K. Panneerselvam, H. H. Freeze, A. Varki, and N. M. Varki. 2001. A novel anionic modification of N-glycans on mammalian endothelial cells is recognized by activated neutrophils and modulates acute inflammatory responses. *J. Immunol.* 166: 624–632.
22. Srikrishna, G., O. Turovskaya, R. Shaikh, R. Newlin, D. Foell, S. Murch, M. Kronenberg, and H. H. Freeze. 2005. Carboxylated glycans mediate colitis through activation of NF-κ B. *J. Immunol.* 175: 5412–5422.
23. Srikrishna, G., H. J. Huttunen, L. Johansson, B. Weigle, Y. Yamaguchi, H. Rauvala, and H. H. Freeze. 2002. N-Glycans on the receptor for advanced glycation end products influence amphoterin binding and neurite outgrowth. *J. Neurochem.* 80: 998–1008.
24. Hofmann, M. A., S. Drury, C. Fu, W. Qu, A. Taguchi, Y. Lu, C. Avila, N. Kambham, A. Bierhaus, P. Nawroth, et al. 1999. RAGE mediates a novel proinflammatory axis: a central cell surface receptor for S100/calgranulin polypeptides. *Cell* 97: 889–901.
25. Ghavami, S., I. Rashedi, B. M. Dattilo, M. Eshraghi, W. J. Chazin, M. Hashemi, S. Wesselborg, C. Kerkhoff, and M. Los. 2008. S100A8/A9 at low concentration promotes tumor cell growth via RAGE ligation and MAP kinase-dependent pathway. *J. Leukocyte Biol.* 83: 1484–1492.
26. Boyd, J. H., B. Kan, H. Roberts, Y. Wang, and K. R. Walley. 2008. S100A8 and S100A9 mediate endotoxin-induced cardiomyocyte dysfunction via the receptor for advanced glycation end products. *Circ. Res.* 102: 1239–1246.
27. Turovskaya, O., D. Foell, P. Sinha, T. Vogl, R. Newlin, J. Nayak, M. Nguyen, P. Nawroth, A. Bierhaus, N. Varki, et al. 2008. RAGE, carboxylated glycans and S100A8/A9 play essential roles in colitis associated carcinogenesis. *Carcinogenesis* epub ahead of print.
28. Sinha, P., V. K. Clements, and S. Ostrand-Rosenberg. 2005. Reduction of myeloid-derived suppressor cells and induction of M1 macrophages facilitate the rejection of established metastatic disease. *J. Immunol.* 174: 636–645.
29. Pulaski, B. A., and S. Ostrand-Rosenberg. 1998. Reduction of established spontaneous mammary carcinoma metastases following immunotherapy with major histocompatibility complex class II and B7.1 cell-based tumor vaccines. *Cancer Res.* 58: 1486–1493.
30. Sinha, P., V. K. Clements, S. K. Bunt, S. M. Albelda, and S. Ostrand-Rosenberg. 2007. Cross-talk between myeloid-derived suppressor cells and macrophages subverts tumor immunity toward a type 2 response. *J. Immunol.* 179: 977–983.
31. Livak, K. J., and T. D. Schmittgen. 2001. Analysis of relative gene expression data using real-time quantitative PCR and the 2(-δ δ C(T)) Method. *Methods* 25: 402–408.
32. Vandal, K., P. Rouleau, A. Boivin, C. Ryckman, M. Talbot, and P. A. Tessier. 2003. Blockade of S100A8 and S100A9 suppresses neutrophil migration in response to lipopolysaccharide. *J. Immunol.* 171: 2602–2609.
33. Goebeler, M., J. Roth, U. Henseleit, C. Sunderkotter, and C. Sorg. 1993. Expression and complex assembly of calcium-binding proteins MRP8 and MRP14 during differentiation of murine myelomonocytic cells. *J. Leukocyte Biol.* 53: 11–18.
34. Hunter, M. J., and W. J. Chazin. 1998. High level expression and dimer characterization of the S100 EF-hand proteins, migration inhibitory factor-related proteins 8 and 14. *J. Biol. Chem.* 273: 12427–12435.
35. Umemura, N., M. Saio, T. Suwa, Y. Kitoh, J. Bai, K. Nonaka, G. F. Ouyang, M. Okada, M. Balazs, R. Adany, et al. 2008. Tumor-infiltrating myeloid-derived suppressor cells are pleiotropic-inflamed monocytes/macrophages that bear M1- and M2-type characteristics. *J. Leukocyte Biol.* 83: 1136–1144.
36. Serafini, P., I. Borrello, and V. Bronte. 2006. Myeloid suppressor cells in cancer: recruitment, phenotype, properties, and mechanisms of immune suppression. *Semin. Cancer Biol.* 16: 53–65.
37. Rossner, S., C. Voigtlander, C. Wiethe, J. Hanig, C. Seifarth, and M. B. Lutz. 2005. Myeloid dendritic cell precursors generated from bone marrow suppress T cell responses via cell contact and nitric oxide production in vitro. *Eur. J. Immunol.* 35: 3533–3544.
38. Movahedi, K., M. Guilliams, J. Van den Bossche, R. Van den Bergh, C. Gysemans, A. Beschin, P. De Baetselier, and J. A. Van Ginderachter. 2008. Identification of discrete tumor-induced myeloid-derived suppressor cell subpopulations with distinct T cell-suppressive activity. *Blood* 111: 4233–4244.
39. Sawanobori, Y., S. Ueha, M. Kurachi, T. Shimaoka, J. E. Talmadge, J. Abe, Y. Shono, M. Kitabatake, K. Kakimi, N. Mukaida, and K. Matsushima. 2008. Chemokine-mediated rapid turnover of myeloid-derived suppressor cells in tumor-bearing mice. *Blood* 1111: 5457–5466.
40. Seth, A., R. Kitching, G. Landberg, J. Xu, J. Zubovits, and A. M. Burger. 2003. Gene expression profiling of ductal carcinomas in situ and invasive breast tumors. *Anticancer Res.* 23: 2043–2051.
41. Carlsson, H., S. Petersson, and C. Enerback. 2005. Cluster analysis of S100 gene expression and genes correlating to psoriasin (S100A7) expression at different stages of breast cancer development. *Int. J. Oncol.* 27: 1473–1481.
42. Arai, K., S. Takano, T. Teratani, Y. Ito, T. Yamada, and R. Nozawa. 2008. S100A8 and S100A9 overexpression is associated with poor pathological parameters in invasive ductal carcinoma of the breast. *Curr. Cancer Drug Targets* 8: 243–252.
43. Hobbs, J. A., R. May, K. Tanousis, E. McNeill, M. Mathies, C. Gebhardt, R. Henderson, M. J. Robinson, and N. Hogg. 2003. Myeloid cell function in MRP-14 (S100A9) null mice. *Mol. Cell. Biol.* 23: 2564–2576.
44. Manitz, M. P., B. Horst, S. Seeliger, A. Strey, B. V. Skryabin, M. Gunzer, W. Frings, F. Schonlau, J. Roth, C. Sorg, and W. Nacken. 2003. Loss of S100A9 (MRP14) results in reduced interleukin-8-induced CD11b surface expression, a polarized microfilament system, and diminished responsiveness to chemoattractants in vitro. *Mol. Cell. Biol.* 23: 1034–1043.
45. Nacken, W., and C. Kerkhoff. 2007. The hetero-oligomeric complex of the S100A8/S100A9 protein is extremely protease resistant. *FEBS Lett.* 581: 5127–5130.
46. Arai, K., T. Teratani, R. Nozawa, and T. Yamada. 2001. Immunohistochemical investigation of S100A9 expression in pulmonary adenocarcinoma: S100A9 expression is associated with tumor differentiation. *Oncol. Rep.* 8: 591–596.
47. Shen, J., M. D. Person, J. Zhu, J. L. Abbruzzese, and D. Li. 2004. Protein expression profiles in pancreatic adenocarcinoma compared with normal pancreatic tissue and tissue affected by pancreatitis as detected by two-dimensional gel electrophoresis and mass spectrometry. *Cancer Res.* 64: 9018–9026.
48. Cross, S. S., F. C. Hamdy, J. C. Deloulme, and I. Rehman. 2005. Expression of S100 proteins in normal human tissues and common cancers using tissue microarrays: S100A6, S100A8, S100A9 and S100A11 are all overexpressed in common cancers. *Histopathology* 46: 256–269.
49. Hermani, A., J. Hess, B. De Servi, S. Medunjanin, R. Grobholz, L. Trojan, P. Angel, and D. Mayer. 2005. Calcium-binding proteins S100A8 and S100A9 as novel diagnostic markers in human prostate cancer. *Clin. Cancer Res.* 11: 5146–5152.
50. Ryckman, C., K. Vandal, P. Rouleau, M. Talbot, and P. A. Tessier. 2003. Proinflammatory activities of S100: proteins S100A8, S100A9, and S100A8/A9 induce neutrophil chemotaxis and adhesion. *J. Immunol.* 170: 3233–3242.
51. Sinha, P., V. K. Clements, S. Miller, and S. Ostrand-Rosenberg. 2005. Tumor immunity: a balancing act between T cell activation, macrophage activation and tumor-induced immune suppression. *Cancer Immunol. Immunother.* 54: 1137–1142.
52. Sica, A., and V. Bronte. 2007. Altered macrophage differentiation and immune dysfunction in tumor development. *J. Clin. Invest.* 117: 1155–1166.
53. Gabrilovich, D. I., V. Bronte, S. H. Chen, M. P. Colombo, A. Ochoa, S. Ostrand-Rosenberg, and H. Schreiber. 2007. The terminology issue for myeloid-derived suppressor cells. *Cancer Res.* 67: 425, author reply 426.
54. Gallina, G., L. Dolcetti, P. Serafini, C. De Santo, I. Marigo, M. P. Colombo, G. Basso, F. Brombacher, I. Borrello, P. Zanovello, et al. 2006. Tumors induce a subset of inflammatory monocytes with immunosuppressive activity on $CD8^+$ T cells. *J. Clin. Invest.* 116: 2777–2790.
55. Huang, B., P. Y. Pan, Q. Li, A. I. Sato, D. E. Levy, J. Bromberg, C. M. Divino, and S. H. Chen. 2006. Gr-1^+CD115^+ immature myeloid suppressor cells mediate the development of tumor-induced T regulatory cells and T-cell anergy in tumor-bearing host. *Cancer Res.* 66: 1123–1131.
56. Yang, R., Z. Cai, Y. Zhang, W. H. Yutzy, K. F. Roby, and R. B. Roden. 2006. CD80 in immune suppression by mouse ovarian carcinoma-associated Gr-1^+CD11b^+ myeloid cells. *Cancer Res.* 66: 6807–6815.
57. Bronte, V., P. Serafini, C. De Santo, I. Marigo, V. Tosello, A. Mazzoni, D. M. Segal, C. Staib, M. Lowel, G. Sutter, et al. 2003. IL-4-induced arginase 1 suppresses alloreactive T cells in tumor-bearing mice. *J. Immunol.* 170: 270–278.
58. Kusmartsev, S., Y. Nefedova, D. Yoder, and D. I. Gabrilovich. 2004. Antigen-specific inhibition of $CD8^+$ T cell response by immature myeloid cells in cancer is mediated by reactive oxygen species. *J. Immunol.* 172: 989–999.
59. Bronte, V., P. Serafini, A. Mazzoni, D. M. Segal, and P. Zanovello. 2003. L-arginine metabolism in myeloid cells controls T-lymphocyte functions. *Trends Immunol.* 24: 302–306.
60. Kusmartsev, S., and D. I. Gabrilovich. 2003. Inhibition of myeloid cell differentiation in cancer: the role of reactive oxygen species. *J. Leukocyte Biol.* 74: 186–196.
61. Pan, P. Y., G. X. Wang, B. Yin, J. Ozao, T. Ku, C. M. Divino, and S. H. Chen. 2008. Reversion of immune tolerance in advanced malignancy: modulation of myeloid-derived suppressor cell development by blockade of stem-cell factor function. *Blood* 111: 219–228.
62. Ohm, J. E., D. I. Gabrilovich, G. D. Sempowski, E. Kisseleva, K. S. Parman, S. Nadaf, and D. P. Carbone. 2003. VEGF inhibits T-cell development and may contribute to tumor-induced immune suppression. *Blood* 101: 4878–4886.
63. Diaz-Montero, C. M., M. L. Salem, M. I. Nishimura, E. Garrett-Mayer, D. J. Cole, and A. J. Montero. 2008. Increased circulating myeloid-derived suppressor cells correlate with clinical cancer stage, metastatic tumor burden, and doxorubicin-cyclophosphamide chemotherapy. *Cancer Immunol. Immunother.* epub ahead of print.
64. Fuellen, G., D. Foell, W. Nacken, C. Sorg, and C. Kerkhoff. 2003. Absence of S100A12 in mouse: implications for RAGE-S100A12 interaction. *Trends Immunol.* 24: 622–624.
65. Suzuki, E., V. Kapoor, A. S. Jassar, L. R. Kaiser, and S. M. Albelda. 2005. Gemcitabine selectively eliminates splenic Gr-1^+/$CD11b^+$ myeloid suppressor cells in tumor-bearing animals and enhances antitumor immune activity. *Clin. Cancer Res.* 11: 6713–6721.